Innovative Infrastructure Solutions (2021) 6:154
https://doi.org/10.1007/s41062-021-00526-9

TECHNICAL PAPER

Mechanical behavior of triple-blended hybrid fiber-reinforced concrete: an experimental and numerical study

Srikanth Koniki[1] · **Hanuma Kasagani**[2] · **Sri Ram Ravi Teja Prathipati**[3] · **Yeswanth Paluri**[3]

Received: 17 February 2021 / Accepted: 22 April 2021

Abstract

Crack growth in concrete gradually increases with an increase in stress levels, and it is a multi-scale process. Concrete reinforced with mono-fibers is effective in improving mechanical properties up to a certain extent. Hybridization of different types of fiber is an alternative solution for early age shrinkage cracks and concrete brittleness. The present investigation aimed to study the mechanical behavior of concrete (50 MPa) reinforced with hybrid graded fibers under uniaxial stress and flexure. Three types of fibers polypropylene, polyester, and hooked-end steel fibers were used for the hybridization. In this study, fibers of different geometry, young's moduli, and tensile strength are selected to investigate the synergy obtained by blending hybrid graded fibers into the concrete. From the experimental results, it was observed that the hybridization of graded fibers into the concrete had achieved superior performance both in strength and stress–strain behavior. An additional nonlinear numerical model was also developed for hybrid fiber-reinforced concrete (HFRC) specimens using finite element-based software (ATENA-GiD) to compare the experimental results. From the experimental and numerical study results, it can be concluded that the addition of hybrid fibers into the concrete improved both the pre-peak and post-peak behavior of the concrete, thereby exhibiting positive synergy in hybridizing metallic and non-metallic fibers into the concrete. Finally, it is observed that there exists a good agreement of results between both the experimental and the numerical study.

Keywords Fiber-reinforced concrete · Hybrid fiber-reinforced concrete · Finite element method · Flexural strength · Stress–strain behavior

Introduction

Concrete with short random discrete fibers can overcome brittleness shortcomings, and early age shrinkage cracks up to a certain level only because fracture in concrete is a multi-scale process [1–6]. Moreover, the fiber effect on concrete depends mainly on fiber aspect ratio, fiber geometry, and tensile strength [7]. Fiber-reinforced concrete (FRC) reinforced with fibers of shorter length or fibers of lower modulus can effectively bridge micro-cracks and improve the composite's tensile strength due to the higher fiber availability in the composite [8]. Concrete reinforced with long length fibers or high-modulus fibers improves the composite's toughness by effectively controlling the growth of micro-cracks into macro-cracks [9]. Hybridization of fibers in the concrete is achieved by combining two or more fibers into the concrete to achieve positive synergy by enhancing the mechanical performance. Every combination might not achieve the synergy effect, and only certain combinations are useful in achieving positive synergy [9, 10]. A successful hybrid fiber-reinforced concrete (HFRC) should succeed in the sum of the mono-FRC results and enhance the concrete's overall performance [11–18].

Polypropylene fibers (PP), in particular, have gained the attention of researchers, mainly due to its ability to arrest shrinkage and micro-cracks formed at lower stress levels. As PP fibers have low modulus, more fibers are available throughout the concrete mix [19, 20]. Polyester fibers (PO) having a density slightly higher than PP can effectively enhance the properties at low and high-stress levels [21].

✉ Yeswanth Paluri
yeswanth.paluri@gmail.com

[1] Department of Civil Engineering, Gokaraju Rangaraju Institute of Engineering and Technology, Bachupally, Hyderabad 500090, India

[2] Department of Civil Engineering, VR-Siddhartha Engineering College, Vijayawada 520007, India

[3] Department of Civil Engineering, Bapatla Engineering College, Bapatla 522101, India

A combination of lower modulus fibers in graded form into the concrete can effectively enhance its performance both at micro- and macro-levels[22]. However, reinforcing concrete with low modulus fibers will not improve the load-carrying capacity at high stress levels[23]. Therefore, the inclusion of high moduli fiber like steel, carbon fibers, etc., into the concrete can control macro-cracks growth at higher stress levels, improve the load-carrying capacity in the failure zone, and improve the toughness of the concrete[9, 24, 25]. However, the addition of higher modulus fibers alone into the concrete will not address the shrinkage and micro-cracks problems due to their lower fiber reinforcing efficiency. A new hybridization system is proposed with blending of lower modulus fibers (PP fiber and PO fiber in the graded form) and higher modulus fibers (hooked-end steel fibers) into the concrete to address the multi-scale cracking developed at varied stress levels in the concrete.

ATENA-GiD, a finite element software, is a user-friendly software used for analytical work, particularly for nonlinear finite element analysis of concrete structures. The actual behavior of concrete structures, cracking, stress–strain behavior, and yielding can be analyzed using ATENA-GiD software [26]. Loading, supports, material definitions, and meshing work were done in ATENA modeling. Two models were generated in the present study, a 200 × 100 × 100 mm small prism for uniaxial compressive stress–strain curve and a 500 × 100 × 100 mm prism for flexure strength. The results from the models developed by ATENA were compared qualitatively and quantitatively with the experimental results.

Research significance

Combining different lengths of fibers in the graded form into the concrete improves the mechanical behavior of concrete, which is taken from the particle packing theory. The main idea is to develop a composite that can utilize the benefits of all the reinforced fibers. The addition of fibers of different moduli into the concrete was investigated in terms of both the material's strength and toughness. Synergy obtained using different types of fibers in the HFRC must be assessed through a number of combinations and trials. It requires a sufficient amount of time and energy for extensive experimentations. To overcome the before said limitation, the nonlinear analysis will be useful. A nonlinear analysis is required particularly for reinforced concrete structures because relatively small deformations and serviceability limitations of the concrete need to be accounted for. The numerical model was developed using ATENA-GiD from the experimental data to simulate the uniaxial behavior of HFRC. The accuracy of the model was further verified with the flexural strength values. In this study, the mechanical performance of the HFRC was successfully investigated experimentally and numerically.

Table 2 Physical properties of fibers used

Fiber property	Polypropylene (PP)	Polyester (PO)	Hooked-end steel fiber (HS)
Length (mm)	6	12	25
Diameter (mm)	0.035	0.044	0.4
Aspect ratio	181	279	62.5
Specific gravity	0.91	1.34	7.84
Elastic modulus (GPa)	4.5	9.5	210

Experimental program

Materials

The properties of various materials used in the present study like cement, fly ash, fine aggregates, coarse aggregate are tabulated in Table 1. The properties of fibers used are tabulated in Table 2.

Table 1 Properties of materials used in the study

Materials	Code	Property/source
Cement (OPC 53 Grade)	IS 12269 [27]	Standard consistency—33% Initial setting time 40 min Final setting time 123 min
Fly ash	IS 3812-Part 1 [28]	Ramagundam thermal power station Specific gravity—2.17
Fine aggregates (FA)	IS 383 [29]	Specific gravity—2.74 Fineness modulus—2.62
Coarse aggregate (CA)	IS 383 [29]	Specific gravity—2.74 Fineness modulus—7.3
Super plasticizer – complast SP430	IS 9103 [30]	FOSROC chemicals Specific gravity—1.18

Table 3 Concrete mix proportions per cubic meter (50 MPa)

Grade of concrete	Cement (kg/m^3)	Fly ash (kg/m^3)	Fine aggregate (kg/m^3)	Coarse aggregate (kg/m^3)	Water (kg/m^3)	Super plasticizer (ml/kg)
50 MPa	400	100	700	1000	196	10

Mix proportions

50 MPa concrete was designed as per Indian standards IS 10262 [31], and the concrete mix proportion is presented in Table 3.

Mixing and curing

A pan mixture of 100 kg capacity was used to mix the ingredients. Cement and mineral admixtures were combined one after the other to get a uniform color. Course and fine aggregates mixed in a pan mixer, then binding materials were transferred to the mixer and mixed for two minutes. Fibers were spread into the mix slowly and then mixed for about 2 min. Water was added slowly to the mixture and mixed for 2 min. Finally, the required amount of super-plasticizer was added to the mix.

Experimental methodology

The experimental work is divided into three phases. The first phase deals with developing non-metallic HFRC consisting of polyester (PO) and polypropylene (PP) fibers in graded form. It has been reported in the literature that a combination of low modulus PP and PO fibers in the ratio of 25% PP + 75% PO give superior performance compared to mono-fibers reinforced concrete [32]. For validation purpose, a hybrid combination of 25% PP + 75% PO at a total fiber volume fractions of 0.1%, 0.15% and 0.2% was considered in the study. And these results were compared with mono-polyester and polypropylene at the same fiber volume fraction. Details of the hybrid combinations and mix designations are presented in Table 4.

The second phase comprises developing metallic and non-metallic HFRC using steel, polyester, and polypropylene fibers. The hybridization concept and hybrid combinations with a 1% fiber dosage are presented in Fig. 1 and Table 5.

The third phase involves validation by developing a nonlinear model using ATENA-GiD software and comparing the experimental data with the numerical results.

Testing methodology

Mechanical properties such as flexural strength (f_{ft}) and compressive strength (f_{ck}) were determined by using Tinius-Olsen Testing Machine of 2000 KN capacity following IS 516 [33]. Uniaxial compressive stress–strain behavior is analyzed by testing prisms of $200 \times 100 \times 100$ mm size in the Tinius-Olsen Testing Machine of 2000 KN capacity. The specimen was kept in a rectangular frame, placed on a 2 MN load cell, and fitted with LVDT's (linearly varying displacement transducers) over a gauge length of 100 mm, as shown in Fig. 2. The LVDTs and load cell were connected to DAC (data acquisition system), as shown in Fig. 3. The specimen was subjected to a gradual increase in load till the failure of

Table 4 Hybrid polypropylene and polyester hybrid combinations and volume percentages

Mix ID	PP (%)	PO (%)	Total fiber volume fraction (%)
PP 0.1	0.1	–	0.1
PP 0.15	0.15	–	0.15
PP 0.2	0.2	–	0.2
PO 0.1	–	0.1	0.1
PO 0.15	–	0.15	0.15
PO 0.2	–	0.2	0.2
NM 0.1	0.025 (25%)	0.075 (75%)	0.1
NM 0.15	0.0375 (25%)	0.1125 (75%)	0.15
NM 0.2	0.05 (25%)	0.15 (75%)	0.2

*Nomenclature

PP 0.1—"PP" Represents the name of the fiber "0.1" percentage of the fiber

NM 0.1—"NM" Denotes the polypropylene – polyester (non-metallic HFRC)

"0.1" Denotes the total fiber volume fraction (25% PP combined with 75% PO to develop Non-metallic HFRC)

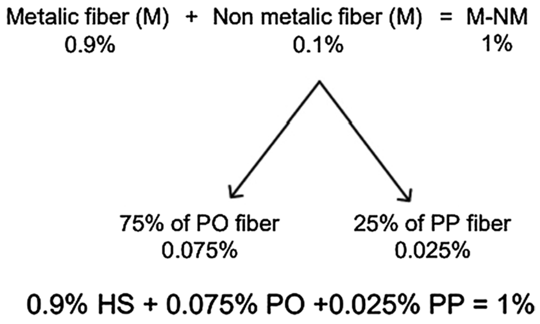

Fig. 1 Example of Hybrid combinations (Metallic–Non-metallic HFRC)

Table 5 Details of steel, polyester, and polypropylene combinations and volume percentages (Metallic and non-metallic HFRC)

Mix ID	Total fiber dosage (%)	Fiber dosage (%)		
		Metallic	Non-metallic (75%-25%)	
		Steel (25 mm)	PO (12 mm)	PP (6 mm)
M-NM 1% (1)	1	0.95	0.05	
M-NM 1% (2)		0.9	0.10	
M-NM 1% (3)		0.85	0.15	
M-NM 1% (4)		0.8	0.20	

*Nomenclature

M-NM 1% (1)

M—Denotes metallic fiber (Hooked-end steel)

NM—Denotes combination of PP and PO (25% PP + 75% PO)

1%—Denotes the total percentage of fiber

(1)—Denotes the percentage of non-metallic fibers replaced with metallic fiber (1)—0.05%, (2)—0.1%, (3)—0.15%, (4)—0.2%

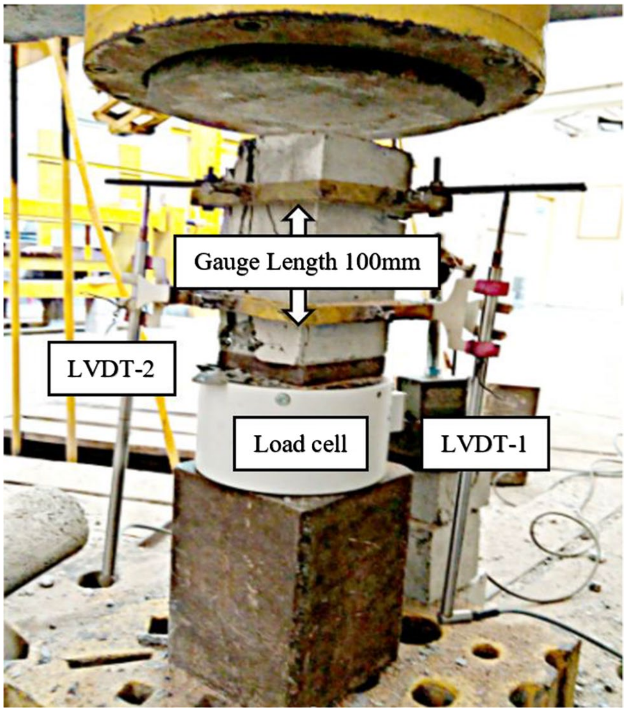

Fig. 2 Testing of prism under uniaxial compression

the specimen, and corresponding loads and deformations were recorded with DAC (data acquisition system).

Concrete's tensile strength can be determined indirectly by using traditional methods like split tensile strength and flexural strength. These techniques work admirably for standard concrete; however, for FRC, it needs a more precise and reliable method [34]. In the present study, a specially designed dog-bone specimen was used to obtain the direct tensile strength and uniaxial tensile stress–strain curve. A schematic diagram of the specimen used for tensile testing with dimensions is shown in Fig. 4. Testing the dog-bone specimen for tensile strength is performed on a 50 KN servo-controlled hydraulic testing frame, and the tensile stress–strain curves are obtained. The experimental setup is presented in Fig. 5.

ATENA-GiD software

ATENA-GiD software, a finite element analysis software, was used for nonlinear analysis exclusively for concrete structures [35]. In the present study, the software is used for simulating the stress–strain behavior of fiber-reinforced concrete numerically. GiD is an interactive tool used for geometric modeling and is used to input data for ATENA analysis. Fiber-reinforced concrete behavior was modeled as nonlinear and having softening branches under uniaxial stress. From the experimental results, the material properties were adopted in the model.

Results and Discussions

Non-metallic HFRC

Basic Mechanical properties of non-metallic HFRC

Mechanical properties and their percentage increase in strength of non-metallic FRC (PP-FRC, PO-FRC), and non-metallic HFRC (PP-PO HFRC) are presented in Table 6. From Table 6, it can be observed that the strength effectiveness of fiber addition in compression is less and mostly insignificant for all mixes. It can also be observed that the increase in tensile properties of concrete is significant with the addition of fibers, which effectively arrests and delays the crack growth. A maximum strength increment of 20.2% in tensile strength and 24.2% in flexural strength is observed at a hybrid combination of 25% PP combined with 75% of PO at a total fiber dosage of 0.2% (NM 0.2). From the results, it can be concluded that the hybridization of non-metallic fibers into the concrete has shown better results compared to addition of mono-fibers into the concrete at the same fiber dosage.

Stress–strain behavior of Non-metallic HFRC under Compression

Uniaxial compressive stress–strain curves of mono-FRC and HFRC consisting of PP and PO fibers are presented

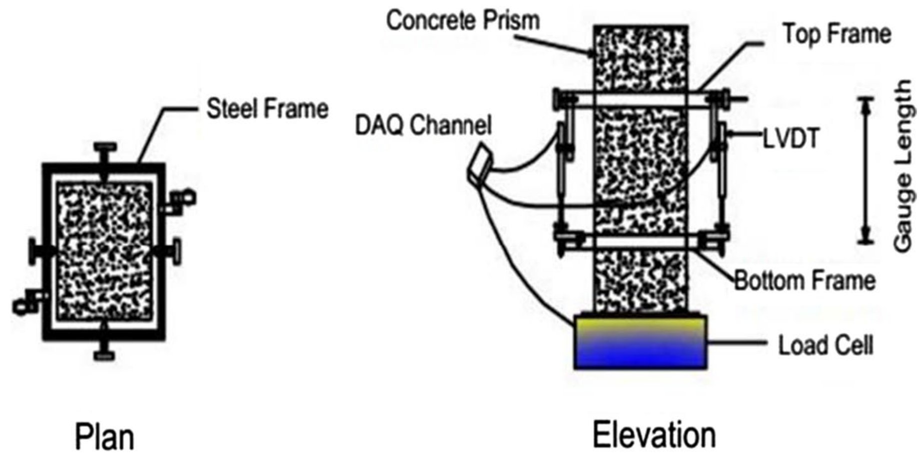

Fig. 3 Schematic diagram of the test setup for uniaxial compression

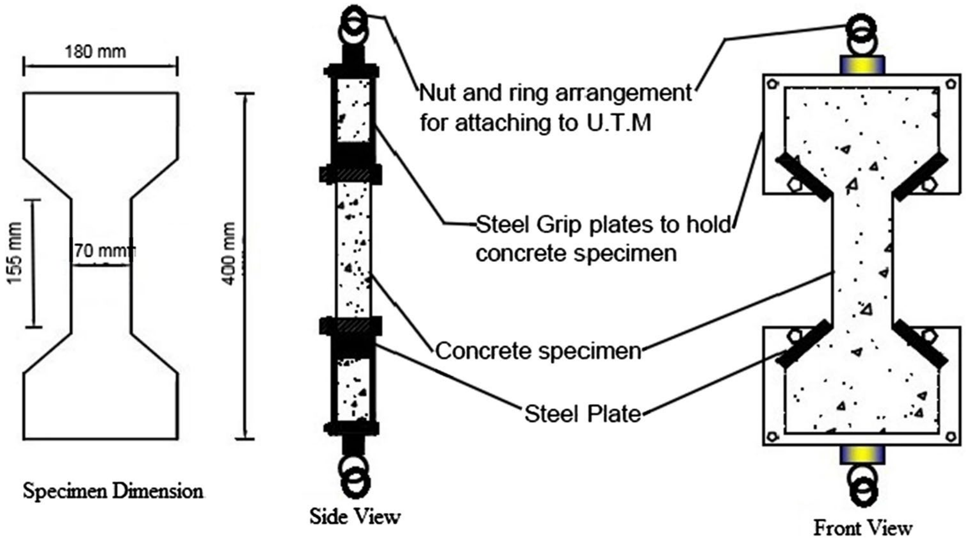

Fig. 4 Schematic diagram of concrete specimen and grip details of direct tensile test

in Fig. 6. Results obtained from stress–strain curves are tabulated in Table 7, from which it can be observed that concrete with mono-fibers did not show significant improvement in the stress–strain behavior of concrete. The reason may be due to the shorter length and lower modulus of PP and PO fibers. However, the influence of hybrid fibers on stress–strain behavior is more promising. Concrete reinforced with a combination of 25% PP and 75% PO produced better performance at all fiber dosages. The maximum strength was achieved at a total fiber dosage of 0.2%, where ductility of HFRC has improved by 30%. It may be attributed to the fact that short and low modulus fibers bridge the cracks at low-stress levels while long fibers control macro-cracks propagation. When compared to mono-FRC, the toughness of concrete (area under the stress–strain curve) increased with fiber hybridization. The maximum value of HFRC is obtained at 0.2% fiber volume and is 2.22. Hybridization of non-metallic fibers (PO and PP) increased the concrete's mechanical properties up to a certain extent only because these fibers are easily pulled out at high stress levels.

Stress–strain behavior of Non-metallic HFRC under Direct Tension

The stress–strain behavior of concrete under uniaxial tension for mono-FRC and HFRC with PP and PO is presented in Fig. 7. The corresponding results are presented in Table 8. The general behavior of concrete under uniaxial tension is such that there is an increase in stress with an increase in strain up to the peak point, and then it fails suddenly. Concrete with mono-fibers (PP and PO) also behaves the same as the control mix and doesn't show any significant improvement in concrete stress–strain behavior. Concrete with hybridized fibers shown strain hardening behavior, i.e., stresses in concrete increased with an increase in strain up to inflection point, then exhibited strain hardening behavior up to the ultimate point and

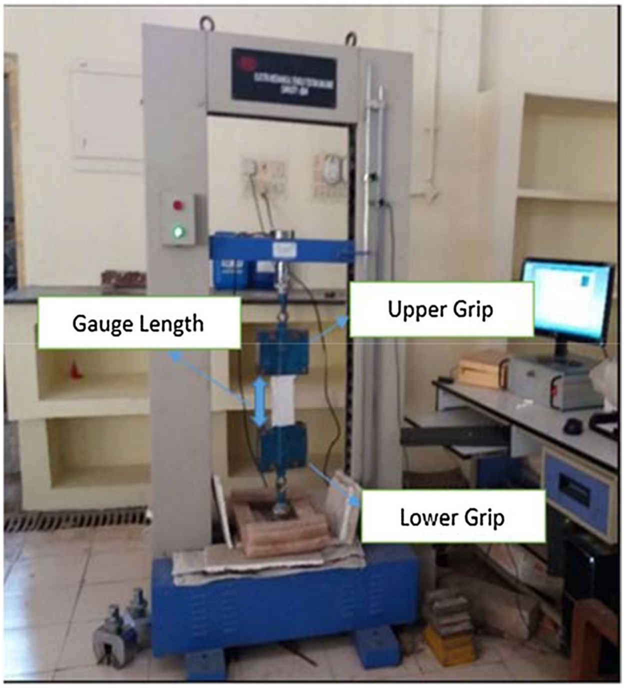

Fig. 5 Direct Tension Test setup

failed abruptly. From the results, it can be noticed that the hybridization of fibers increased the ductility of concrete under tension. The percentage increase in stress at inflection is maximum at 0.2% (75% PO + 25% PP) which is about 11.2%. The increase in stress at the inflection point may be due to fibers' contribution in arresting micro-crack. However, there is no significant improvement in concrete post-peak behavior as non-metallic fibers are effective only at low stress levels.

Metallic–Non-metallic HFRC

HFRC with a combination of PP and PO improved concrete properties at low-stress levels only, and at high-stress levels, these are not promising in controlling the growth of macro-cracks because of the shorter length and lower modulus of these fibers. To increase the properties at high stress levels, long and high modulus steel fibers were introduced.

Basic mechanical properties of Metallic–Non-metallic HFRC

Mechanical properties of mono-FRC and HFRC at a fiber dosage of 1% are presented in Table 9. From Table 9, it can be noted that HFRC with steel and non-metallic fibers has shown better performance as compared to control and mono-FRC at the same fiber volume fraction. This may be due to a combination of short and long fibers with low and high modulus, which arrested the crack propagation both at low- and high-stress levels. The maximum strength was achieved at M-NM 1 (3), a combination of steel 0.85% metallic and non-metallic fiber of 0.15%. The strength improvement of HFRC at optimum dosage is 9.1% in compression, 39.5% in direct tension, and 46.2% in flexure. From Table 9, it can also be observed that there is a decrease in strength values when concrete was reinforced with non-metallic fibers above optimum dosage, i.e., at M-NM 1 (4). This may be due to the higher availability of non-metallic fiber in the mix, which leads to low workability and improper compaction.

Table 6 Mechanical properties and their corresponding strength effectiveness of mono-FRC and HFRC

Mix ID	f_{ck}	% Increase	f_{dt}	% Increase	f_{ft}	% Increase
CM	58.0	–	4.63	–	5.42	–
PP 0.1	58.9	1.5	4.93	6.6	6.09	12.4
PP 0.15	**59.2**	**2.1**	**5.11**	**10.3**	**6.17**	**13.7**
PP 0.2	58.6	1.1	5.02	8.2	5.93	9.4
PO 0.1	58.7	1.3	5.12	10.7	6.15	13.4
PO 0.15	**59.1**	**2.0**	**5.24**	**13.2**	**6.36**	**17.4**
PO 0.2	58.8	1.5	5.15	11.3	5.96	6.62
NM 0.1	59.0	1.8	5.3	14.6	6.5	19.0
NM 0.15	59.3	2.3	5.4	17.7	6.6	21.0
NM 0.2	**59.5**	**2.6**	**5.6**	**20.2**	**6.7**	**24.2**

*Nomenclature

f_{ck}—Compressive strength, f_{dt}—Direct tensile strength, f_{ft}—flexural strength

Bold indicates optimum dosage where the percentage improvement is maximum

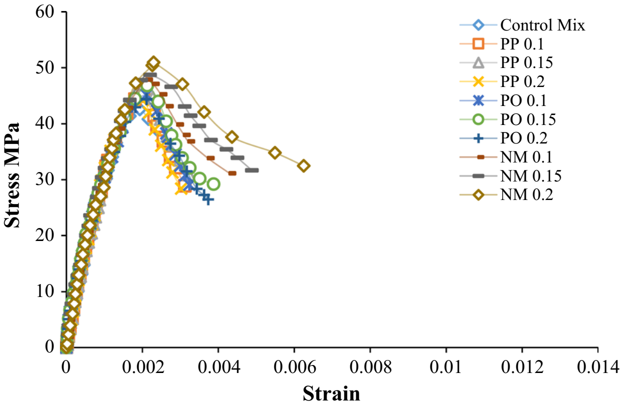

Fig. 6 Uniaxial compressive stress–strain curves of mono-FRS and HFRC

Stress–strain behavior of Metallic–Non-metallic HFRC under Compression

Stress–strain curves of HFRC under compression are shown in Fig. 8, and the results obtained from curves are presented in Table 10. From Table 10, it is observed that the hybridization of metallic fiber with non-metallic fibers improved the stress–strain behavior of the concrete. The improvement in strength and toughness may be due to the effectiveness of short and low modulus fibers (PO and PP) in the bridging of cracks developed at low-stress levels, thereby improving the peak strength. Maximum improvement in peak strength of 9.1% observed at 0.85% metallic + 0.15% non-metallic hybrid combination. At high-stress levels, the low modulus fibers cannot resist the load, and stresses in concrete are resisted by steel fibers by controlling the development of macro-cracks thereby increasing the post-peak toughness. The failure strain of the concrete also increased with fiber hybridization. A maximum failure strain of 31.2 × 10–2 is observed at a hybrid combination of M-NM 1 (3). From Table 10, it can be observed that the ductility of concrete also increased; this may be due to the positive interaction between metallic and non-metallic fibers.

Stress–strain behavior of Metallic–Non-metallic HFRC under Direct Tension

Stress–strain curves of HFRC under direct tension are presented in Fig. 9, and the corresponding results of the stress–strain curve are shown in Table 11. From the results, it can be noted that there is an improvement in both pre- and post-peak behavior of stress–strain curve with fiber hybridization when compared to mono-fibers of the same fiber dosage. It is also observed that the curve shows a strain hardening behavior up to the ultimate point,

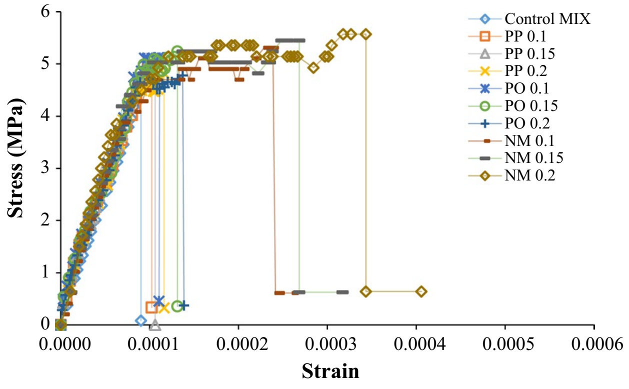

Fig. 7 Stress–strain curves of HFRC under direct tension

Table 7 Stress–strain properties of PO-PP HFRC under compression

Mix ID	σ^c_u (MPa)	% Increase	$\varepsilon^c_u \times 10^{-2}$	$E_s \times 10^3$ (MPa)	D_f	EA^c	T_f
CM	42.59	–	19.3	33.83	2.21	0.0979	1
PP 0.1	57.84	5.8	20.2	46.08	2.21	0.1486	1.29
PP 0.15	59.63	9.1	20.1	46.12	2.24	0.1606	1.39
PP 0.2	55.73	2.0	20.1	46.01	2.22	0.1500	1.30
PO 0.1	57.63	5.5	22.0	46.64	2.26	0.1598	1.39
PO 0.15	59.81	9.4	22.3	46.80	2.31	0.1857	1.61
PO 0.2	56.01	2.5	21.3	46.81	2.41	0.1706	1.48
NM 0.1	47.87	12.4	21.1	36.41	2.42	0.1543	1.58
NM 0.15	48.70	14.3	22.1	37.24	2.75	0.1754	1.79
NM 0.2	49.95	17.3	23.0	38.85	3.02	0.2178	2.22

Table 8 Stress–strain properties of PO-PP HFRC under direct tension

Mix Id	σ^t_f (MPa)	$\varepsilon^t_f \times 10^{-5}$	σ^t_u (MPa)	$\varepsilon^t_b \times 10^{-5}$	$EA^t \times 10^{-5}$ (MPa)
Control mix	4.63	9.02	4.63	9.02	63.0
PP 0.1	4.78	9.15	4.93	9.7	67.9
PP 0.15	4.83	9.23	5.11	10.1	74.0
PP 0.2	4.65	10.8	5.01	11.0	78.1
PO 0.1	4.86	8.99	5.12	10.0	71.0
PO 0.15	4.93	9.26	5.24	11.3	85.2
PO 0.2	4.64	8.95	5.15	13.9	92.8
NM 0.1	4.92	10.2	5.3	17.1	128.42
NM 0.15	5.12	9.54	5.44	16.9	121.24
NM 0.2	5.21	11.21	5.57	22.8	165.48

Table 9 Mechanical properties of metallic and non-metallic HFRC

Mix ID	f_{ck}	% Increase	f_{dt}	% Increase	f_{ft}	% Increase
CM	58.0	–	4.63	–	5.42	–
HS 1	61.2	5.6	5.49	18.6	6.59	21.6
M-NM 1 (1)	61.3	5.8	6.23	34.7	7.5	38.0
M-NM 1 (2)	62.5	7.9	6.36	37.5	7.8	43.0
M-NM 1 (3)	63.2	9.1	6.46	39.5	7.9	46.2
M-NM 1 (4)	59.5	2.6	5.95	28.5	6.6	22.1

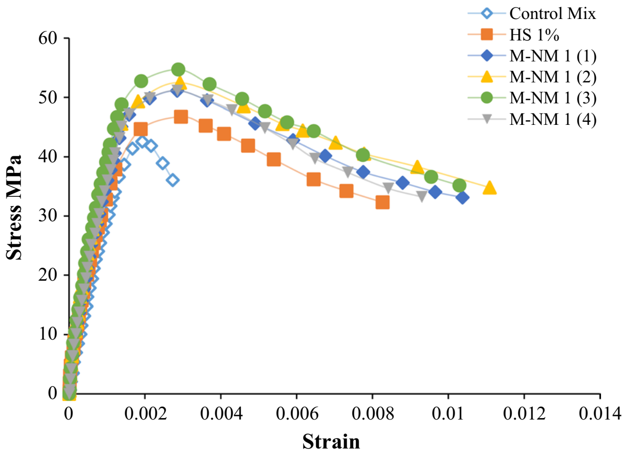

Fig. 8 Stress–strain curves of HFRC under uniaxial compression

followed by a small amount of strain softening, and then failed abruptly. Strain at breaking point also increased significantly with the hybridization of fibers. The maximum increment in failure strain is 346% at a hybrid combination of M-NM 1 (3). From the results, it can be inferred that the hybridization of steel fiber with a small amount of non-metallic fiber would significantly improve the mechanical behavior of concrete.

Results and Discussion of numerical modeling by ATENA

ATENA-GiD is a finite element analysis software exclusively for nonlinear analysis of concrete structures. To develop an HFRC with an optimum dosage, one needs to go through more combinations and has to perform many trials that require more time and energy. ATENA-GiD software

Table 10 Stress–strain properties of HFRC under compression

Mix ID	σ^c_u (MPa)	% Increase	$\varepsilon^c_u \times 10^{-2}$	$E_s \times 10^3$ (MPa)	D_f	EA^c	T_f
CM	42.59	–	19.3	33.83	2.21	0.0979	1
HS 1	46.76	9.8	29.5	38.97	3.32	0.2709	2.77
M-NM 1 (1)	51.11	20.0	30.6	45.36	3.94	0.3215	3.28
M-NM 1 (2)	52.47	23.2	30.9	49.83	3.99	0.3484	3.56
M-NM 1 (3)	54.68	28.4	31.2	50.98	4.12	0.3417	3.49
M-NM 1 (4)	51.15	20.1	30.0	50.98	3.57	0.2982	3.04

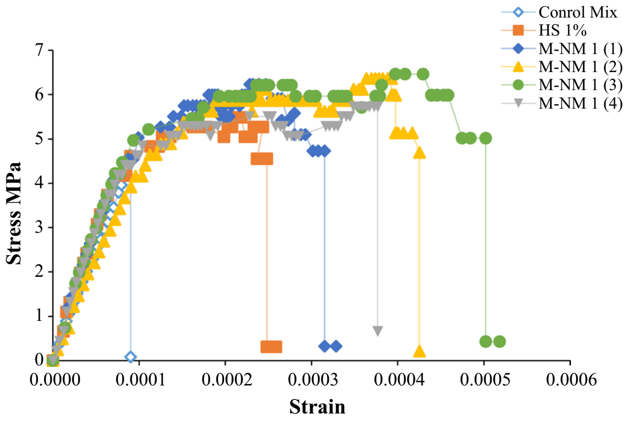

Fig. 9 Stress–strain curves of HFRC under direct tension

was used to develop a nonlinear model, and this model was validated with experimental results.

FEM Model Generation

ATENA-GiD was used to develop a 200 × 100 × 100 mm model. Input parameters were taken as experimental results of compressive strength, direct tensile strength, and stress–strain values. This was due to the limitation to give hybrid fibers (three fibers) as input parameters to model in ATENA. To determine the stress–strain behavior under compression, prism of dimensions 200 × 100x100 mm was analyzed to check the accuracy of the model, and then with the same input data, flexure specimen of 500 × 100x100 mm prism was analyzed in ATENA-GiD software for validation. The shape of the present study's element is hexahedron for concrete specimens and tetrahedron for supporting steel plates. The boundary conditions used in the analysis were the same as that of the simply supported beam. Steps involved in the modeling of the 200 × 100x100 mm specimen are shown in Fig. 10. For concrete under uniaxial compression, the experimental stress–strain curves for 50 MPa concrete and the stress–strain curves generated by ATENA model are presented in Fig. 11. Table 12 shows the comparison of results between both experimental and ATENA model. When compared to the experimental peak stress values, the ATENA software model values are on the higher side. It is also observed that values obtained through the ATENA model are in good agreement with experimental values, while the percentage error found in peak-stress is not more than 15%. A similar trend was also observed in toughness values.

Modeling of 500 × 100x100mm Prism for flexure:

A flexural model of 500 × 100 × 100 mm was developed to validate the ATENA model with experimental results with the properties obtained from the compression model, i.e., 200 × 100 × 100 mm specimen. For the flexural model, only half of the portion was considered and analyzed in ATENA because it is symmetrical on both sides from the center of the specimen. The steps to develop a model are presented in Fig. 12. To generate a hybrid fiber-reinforced concrete model, the experimental stress–strain curve obtained for concrete under uniaxial stress is given manually. A comparison of ATENA results with experimental results is presented in Table 13. From the values, it is observed that the predicted flexural strength values are in good agreement with experimental results. The percentage error is not more than 10%.

Conclusions

From the experimental and numerical investigation on the mechanical behavior of HFRC, the following conclusions were drawn and presented:

Table 11 Strength properties of stress–strain curve under direct tension

Mix Id	σ^t_f (MPa)	$\varepsilon^t_f \times 10^{-5}$	σ^t_u (MPa)	$\varepsilon^t_b \times 10^{-5}$	$EA^t \times 10^{-5}$ (MPa)
CM	4.63	9.02	4.63	9.02	63.0
HS 1	5.27	11.25	5.49	25.9	181.6
M-NM 1 (1)	5.29	11.29	6.23	32.9	263.2
M-NM 1 (2)	5.32	11.36	6.36	42.5	361.4
M-NM 1 (3)	5.34	11.34	6.46	51.8	392.8
M-NM 1 (4)	5.22	11.27	5.95	37.4	276.2

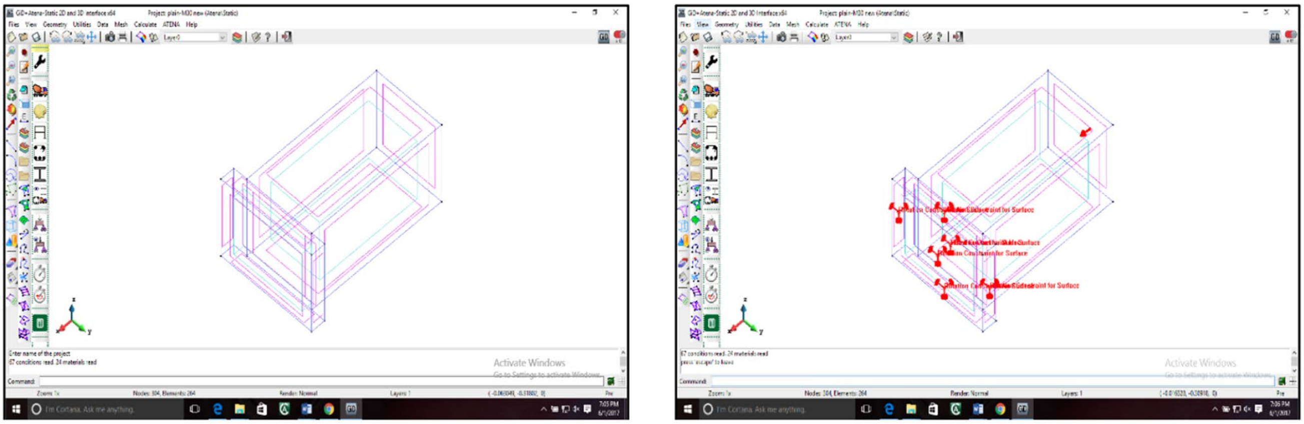

(a) Geometric model in ATENA-GiD **(b)** After imposing boundary conditions

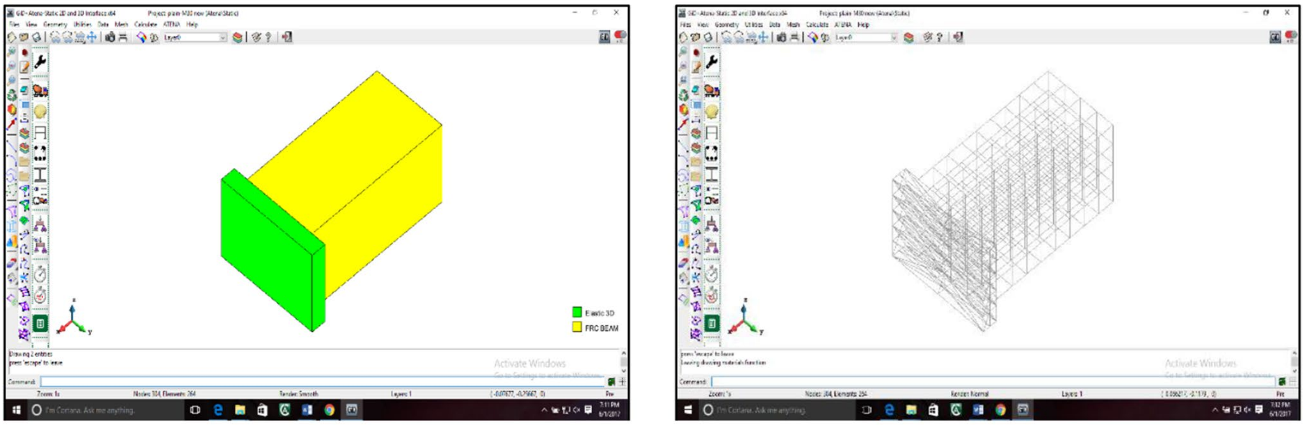

(c) Model after assigning material properties **(d)** Meshing of Prism and Plates

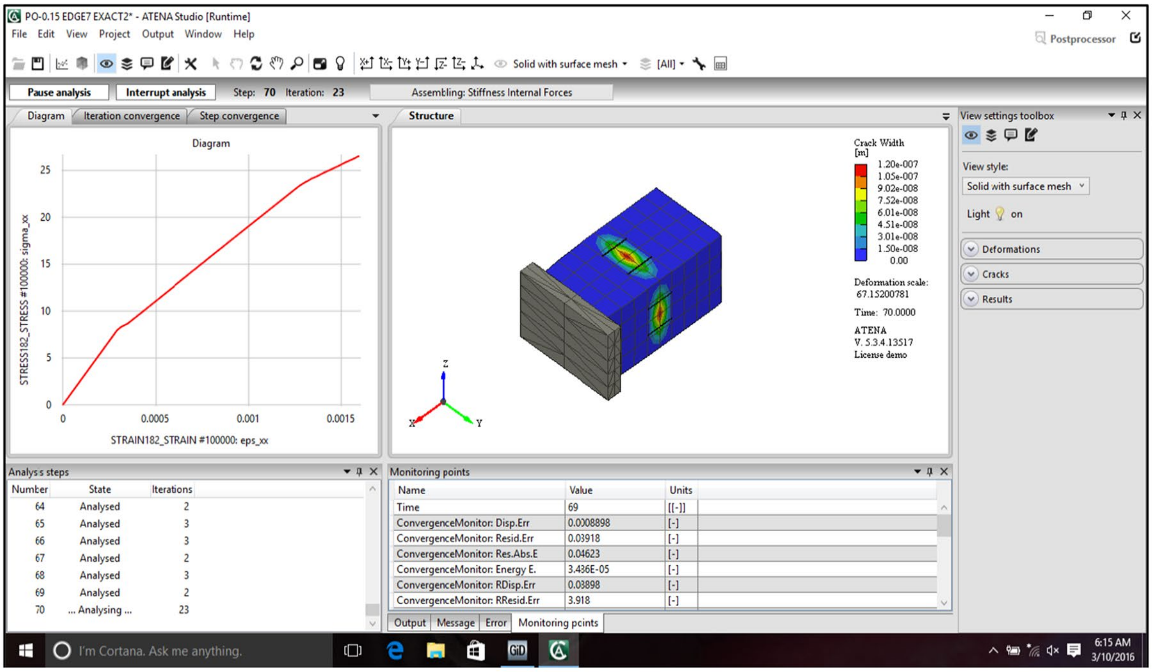

Step: 70 Iteration: 23

Assembling: Stiffness Internal Forces

Deformation scale: 67.15200781

Time: 70.0000

ATENA
V. 5.3.4.13517
License demo

Analysis steps

Number	State	Iterations
64	Analysed	2
65	Analysed	3
66	Analysed	3
67	Analysed	2
68	Analysed	3
69	Analysed	2
70	... Analysing ...	23

Monitoring points

Name	Value	Units
Time	69	[[-]]
ConvergenceMonitor: Disp.Err	0.0008898	[-]
ConvergenceMonitor: Resid.Err	0.03918	[-]
ConvergenceMonitor: Res.Abs.E	0.04623	[-]
ConvergenceMonitor: Energy E.	3.436E-05	[-]
ConvergenceMonitor: RDisp.Err	0.03898	[-]
ConvergenceMonitor: RResid.Err	3.918	[-]

(e) Stress contours due to direct compression

Fig. 10 Modeling of 200 × 100 × 100 mm in ATENA

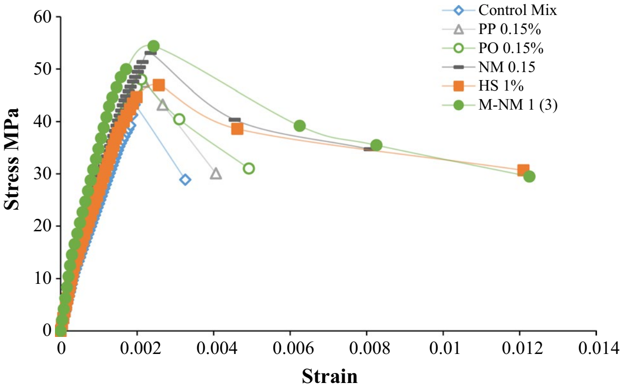

Fig. 11 ATENA Model stress–strain curves of mono and HFRC under uniaxial compression test

- There was a marginal improvement in the compressive strength values for HFRC mixes. However, a significant improvement in tensile strength values was observed for HFRC mixes, which might be due to the effectiveness of fibers in the concrete under uniaxial tension.
- HFRC developed by blending PP and PO fibers exhibited better strength and toughness properties than their mono-counterparts and control mix.
- Grading of PO and PP fibers is effective, and the combination of 75% of PO fiber combined with 25% of PP fiber into the concrete is considered as the best mix in the study.
- A positive synergy in HFRC is observed by replacing metallic fibers with a partial replacement of 0.15% of graded non-metallic fibers into the concrete.
- From both the experimental and numerical study, it was observed that hybridization of steel, polyester, and polypropylene significantly enhanced both pre-peak and post-peak performance of the composite.
- Comparison of the strength and toughness values from the experimental results and numerical study reveals that the percentage error was within 15%.
- A numerical study using finite element software, ATENA-GiD, is validated for the experimental flexural strength values of HFRC. The results obtained from the numerical model and experimental program are in good agreement with less than 10% error.

From this study, it can be understood that utilization of fly ash as a supplementary cementitious material in combination with hybrid fibers (metallic + non-metallic) is proved to be advantageous in improving the mechanical performance, thereby considered as a sustainable alternative to normal concrete reinforced with mono-fibers. It can also be inferred that FEM software ATENA can be successfully employed in the validation of the experimental work, thereby reducing the effort and resources required in the optimization of the experimental study.

Table 12 Comparison of experimental and ATENA for 50 MPa concrete

Mix ID	Peak stress			Toughness		
	Experimental	Analytical	Error (%)	Experimental	Analytical	Error (%)
Control Mix	42.59	43.25	1.53%	0.098	0.1125	14.91%
PP 0.15%	47.08	49.56	5.00%	0.130	0.1574	21.26%
PO 0.15%	46.8	50.00	6.40%	0.142	0.1452	2.18%
NM 0.15%	49.95	53.06	5.86%	0.218	0.2552	17.17%
HS 1%	46.76	52.12	10.28%	0.271	0.3246	19.83%
M-NM 3 (1)	54.68	54.38	-0.55%	0.298	0.2832	-5.03%

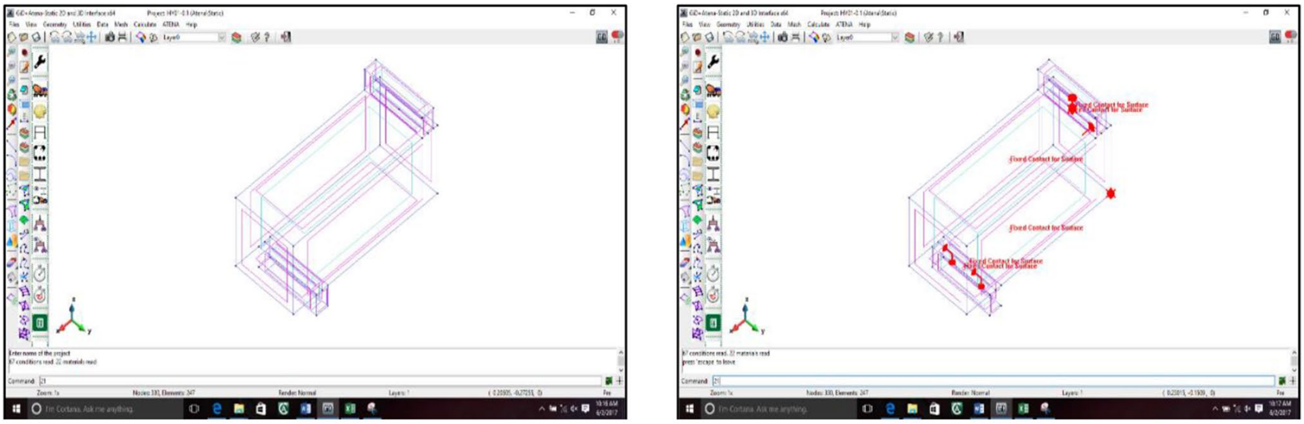

(a) Geometric model in ATENA-GiD **(b)** After imposing boundary conditions

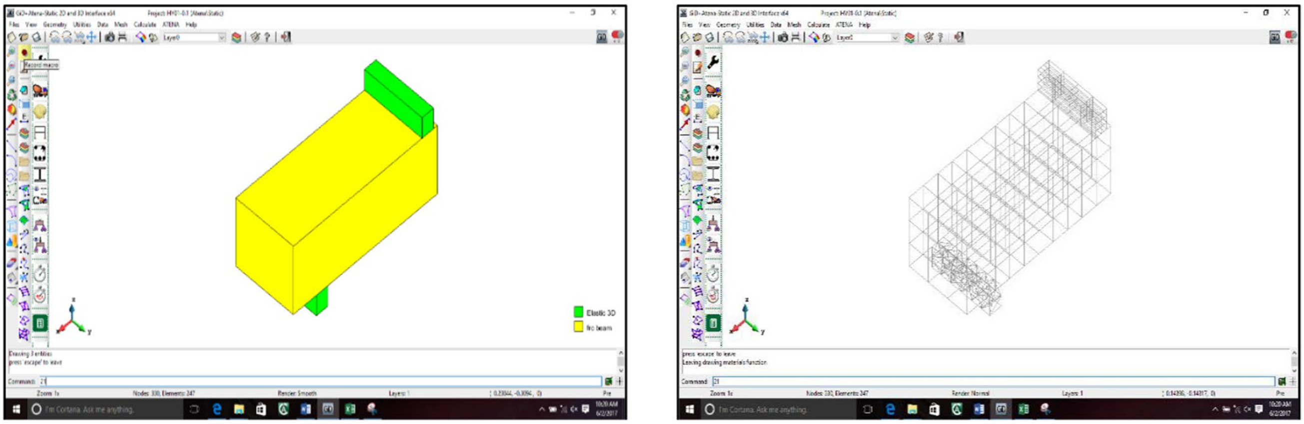

(c) Model after assigning material properties **(d)** Meshing of Prism and Plates

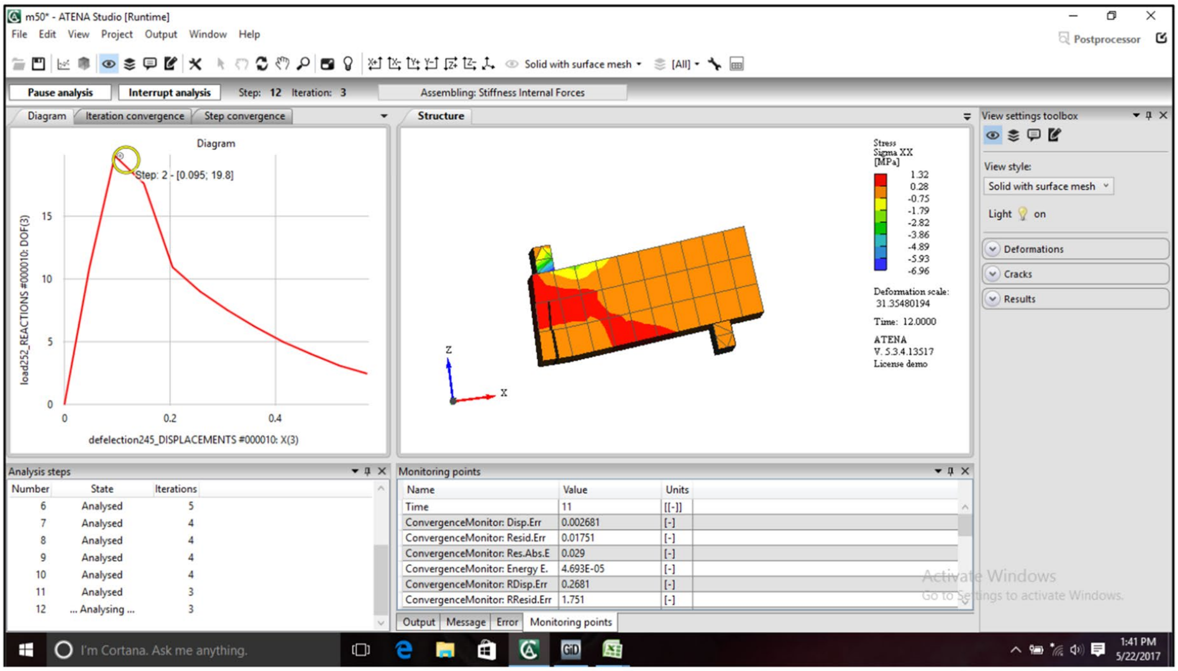

Step: 12 Iteration: 3

Assembling: Stiffness Internal Forces

View style: Solid with surface mesh

Light on

Deformation scale: 31.35480194

Time: 12.0000

ATENA
V. 5.3.4.13517
License demo

Analysis steps

Number	State	Iterations
6	Analysed	5
7	Analysed	4
8	Analysed	4
9	Analysed	4
10	Analysed	4
11	Analysed	3
12	... Analysing ...	3

Monitoring points

Name	Value	Units
Time	11	[[-]]
ConvergenceMonitor: Disp.Err	0.002681	[-]
ConvergenceMonitor: Resid.Err	0.01751	[-]
ConvergenceMonitor: Res.Abs.E	0.029	[-]
ConvergenceMonitor: Energy E.	4.693E-05	[-]
ConvergenceMonitor: RDisp.Err	0.2681	[-]
ConvergenceMonitor: RResid.Err	1.751	[-]

(e) Stress contours due to flexure loading

Fig. 12 Modeling of 500 × 100 × 100 mm

Table 13 Comparison of experimental and ATENA flexure strength values 50 MPa

Mix ID	Experimental flexure strength (MPa)	Analytical flexure strength (MPa)	Error (%)
Control Mix	5.42	5.43	−0.18
PP 0.15	6.17	6.48	−5.02
PO 0.15	6.36	6.93	−8.96
M-NM 0.2 (3)	6.73	6.33	5.94
HS 0.5%	6.25	6.38	−2.08
HS 0.75%	6.37	6.31	0.94
HS 1%	6.59	5.93	10.02
M-NM 0.5 (3)	7.38	8.12	−10.03
M-NM 0.75 (3)	7.7	7.55	1.95
M-NM 1 (3)	7.93	7.85	1.01

Acknowledgment The authors would like to thank the Department of Civil engineering, National Institute of Technology Warangal, for providing research facilities to carry out this research work.

Declaration

Conflict of interest On behalf of all authors, the corresponding author states that there is no conflict of interest.

References

1. Committee A (2008) State-of-the-art report on fiber reinforced concrete-ACI 544.1 R-96 (Reapproved 2002). ACI manual of concrete practice, Part.6
2. Shah SP (1985) Fracture toughness of fiber reinforced concrete. In: Northwestern Univ Evanston IL DEPT OF CIVIL ENGINEERING
3. Van Mier J, Vonk R (1991) Fracture of concrete under multiaxial stress-recent developments. Mater Struct 24(1):61–65
4. Paluri Y, Mogili S, Mudavath H, Pancharathi RK (2020) A study on the influence of steel fibers on the performance of Fine Reclaimed Asphalt Pavement (FRAP) in pavement quality concrete. Mater Today Proc 32:657–662
5. Vijay K, Murmu M (2019) Self-repairing of concrete cracks by using bacteria and basalt fiber. SN Appl Sci 1(11):1–10
6. Paluri Y, Noolu V, Mudavath H, Kumar PR (2021) Flexural fatigue behavior of steel fiber-reinforced reclaimed asphalt pavement-based concrete: an experimental study. Pract Period Struct Des Constr 26(1):04020053
7. Hannawi K, Bian H, Prince-Agbodjan W, Raghavan B (2016) Effect of different types of fibers on the microstructure and the mechanical behavior of ultra-high performance fiber-reinforced concretes. Compos B Eng 86:214–220
8. Banthia N, Gupta R (2004) Hybrid fiber reinforced concrete (HyFRC): fiber synergy in high strength matrices. Mater Struct 37(10):707–716
9. Banthia N, Sappakittipakorn M (2007) Toughness enhancement in steel fiber reinforced concrete through fiber hybridization. Cem Concr Res 37(9):1366–1372
10. AloopDE N (2020) Experimental and analytical study of the mechanical and flexural behavior of hybrid fiber concretes. Structures 28:1746–1755
11. Teng S, Afroughsabet V, Ostertag CP (2018) Flexural behavior and durability properties of high performance hybrid-fiber-reinforced concrete. Constr Build Mater 182:504–515
12. Wang D, Ju Y, Shen H, Xu L (2019) Mechanical properties of high performance concrete reinforced with basalt fiber and polypropylene fiber. Constr Build Mater 197:464–473
13. Kasagani H, Rao CBK (2018) Effect of graded fibers on stress strain behaviour of glass fiber reinforced concrete in tension. Constr Build Mater 183:592–604. https://doi.org/10.1016/j.conbuildmat.2018.06.193
14. Niu DT, Huang DG, Fu Q (2019) Experimental investigation on compressive strength and chloride permeability of fiber-reinforced concrete with basalt-polypropylene fibers. Adv Struct Eng 22(10):2278–2288. https://doi.org/10.1177/1369433219837387
15. Prathipati ST, Rao C (2021) A study on the uniaxial compressive behaviour of graded fiber reinforced concrete using glass fiber/steel fiber. Innovative Infrastruct Sol 6(2):1–14
16. Teja Prathipati S, Rao C, Dakshina MN (2020) Mechanical behavior of hybrid fiber reinforced high strength concrete with graded fibers. Int J Eng 33(8):1465–1471
17. Kasagani H, Teja Prathipati SRR, Rao CBK (2020) Influence of graded glass fibres on strain hardening and strain softening behaviour of CGGF under uniaxial stress. Mag Concrete Res.1–27
18. Prathipati ST, Rao C (2020) A study on the uniaxial behavior of hybrid graded fiber reinforced concrete with glass and steel fibers. Mater Today PROC 32:764–770
19. Afroughsabet V, Biolzi L, Monteiro PJ (2018) The effect of steel and polypropylene fibers on the chloride diffusivity and drying shrinkage of high-strength concrete. Compos B Eng 139:84–96
20. Alhozaimy AM, Soroushian P, Mirza F (1996) Mechanical properties of polypropylene fiber reinforced concrete and the effects of pozzolanic materials. Cement Concr Compos 18(2):85–92. https://doi.org/10.1016/0958-9465(95)00003-8
21. Gupta S, Rao VK, Sengupta J (2008) Evaluation of polyester fiber reinforced concrete for use in cement concrete pavement works. Road Mater Pavement Des 9(3):441–461
22. Koniki S, Ravi P (2018) A study on mechanical properties and stress-strain response of high strength concrete reinforced with polypropylene–polyester hybrid fibres. Cement Wapno Beton 1:67–77
23. Afroughsabet V, Ozbakkaloglu T (2015) Mechanical and durability properties of highstrength concrete containing steel and polypropylene fibers. Constr Build Mater 94:73–82. https://doi.org/10.1016/j.conbuildmat.2015.06.051
24. Koniki S, Prasad DR (2019) Mechanical properties and constitutive stress–strain behaviour of steel fiber reinforced concrete under uni-axial stresses. J Build Pathol Rehabil 4(1):6
25. Qian C, Stroeven P (2000) Development of hybrid polypropylene-steel fibre-reinforced concrete. Cem Concr Res 30(1):63–69
26. Kannam P, Sarella VR (2018) A study on validation of shear behaviour of steel fibrous SCC based on numerical modelling (ATENA). J Build Eng 19:69–79
27. IS:12269–2013. Ordinary portland cement 53 grade-specifications. Bureau of Indian Standards, New Delhi, India; 2013.
28. IS:3812-Part:1–2003 (2013) Specification for pulverized fuel ash, Part 1: For Use as Pozzolana in Cement, Cement mortar and concrete. Bureau of Indian Standards New Delhi
29. IS:383–1970 (1970) Indian standard specification for coarse and fine aggregates from natural sources for concrete. Bureau of Indian Standards, New Delhi

30. IS:9103–1999 (1999) Standard specification for chemical admixtures for concrete. Bureau of Indian Standards, New Delhi
31. IS:10262–2019 (2019) Concrete mix proportioning–guidelines. Bureau of Indian Standards, New Delhi
32. Koniki S, Prasad DR (2019) Influence of hybrid fibres on strength and stress-strain behaviour of concrete under uni-axial stresses. Constr Build Mater 207:238–248. https://doi.org/10.1016/j.conbuildmat.2019.02.113
33. IS:516–1959 (2018). Methods of test for strength of concrete. Bureau of Indian Standards, New Delhi
34. Naaman AE, Reinhardt H-W (2006) Proposed classification of HPFRC composites based on their tensile response. Mater Struct 39(5):547–555
35. Cervenka V, Cervenka J, Pukl R (2002) ATENA—A tool for engineering analysis of fracture in concrete. Sadhana 27(4):485–492